Proceedings of the ASME 2009 Dynamic Systems and Control Conference
DSCC2009
October 12-14, 2009, Hollywood, California, USA

DSCC2009-2507

A HYBRID OPTIMAL CONTROL STRATEGY FOR A SMART PROSTHETIC HAND

Cheng-Hung Chen
Measurement and Control
Engineering Research Center
Department of Biological Sciences
Idaho State University
Pocatello, Idaho 83209
Email: chenchen@isu.edu

D. Subbaram Naidu
Measurement and Control
Engineering Research Center
Department of Electrical Engineering
Idaho State University
Pocatello, Idaho 83209
Email: naiduds@isu.edu

Alba Perez-Gracia
Measurement and Control
Engineering Research Center
Department of Mechanical Engineering
Idaho State University
Pocatello, Idaho 83209
on leave with Institut de Robotica i
Informatica Industrial (UPC-CSIC)
c/ Llorens i Artigas 4-6
Barcelona, Spain
Email: perealba@isu.edu

Marco P. Schoen
Measurement and Control
Engineering Research Center
Department of Mechanical Engineering
Idaho State University
Pocatello, Idaho 83209
Email: schomarc@isu.edu

ABSTRACT

This paper presents a hybrid of a soft computing or control technique of adaptive neuro-fuzzy inference system (ANFIS) and a hard computing or control technique of the hybrid finite-time linear quadratic optimal control for a two-fingered (thumb and index) prosthetic hand. In particular, the ANFIS is used for inverse kinematics, and the optimal control is used to minimize tracking error utilizing feedback linearized dynamics. The simulations of this hybrid controller, when compared with the proportional-integral-derivative (PID) controller showed enhanced performance. Work is underway to extend this methodology to a five-fingered, three-dimensional prosthetic hand.

NOMENCLATURE

$p_d^j(t)$ Desired fingertip positions of j finger (j=t, i, m, r and l)
$v_d^j(t)$ Desired fingertip velocities
$a_d^j(t)$ Desired fingertip accelerations
A_i Undetermined constants ($i = 0-3$)
t_0 Initial time
t_f Terminal time
(X^t,Y^t) Fingertip coordinate of thumb (t)
L_k^t The length of the link $k(=1,2)$ of thumb (t)
q_k^t The angle of the joint $k(=1,2)$ of thumb (t)
$\mathbf{J^t}$ The *Jacobian* of thumb
$\dot{q}_k^t$ The angular velocities of the joint $k(=1,2)$ of thumb
$\ddot{q}_k^t$ The angular accelerations of the joint $k(=1,2)$ of thumb
(X^i,Y^i) Fingertip coordinate of index finger (i)
q_k^i The length of the link $k(=1,2,3)$ of index finger (i)
L_k^i The angle of the joint $k(=1,2,3)$ of index finger (i)
$\mathbf{J^i}$ The *Jacobian* of index finger
$\dot{q}_k^i$ The angular velocities of the joint $k(=1,2,3)$ of index finger
$\ddot{q}_k^i$ The angular accelerations of the joint $k(=1,2,3)$ of index finger
$\mathcal{L}$ Lagrangian
$\dot{\mathbf{q}}$ The angular velocity vector of joints

$\mathbf{q}$ The angle vector of joints
$\boldsymbol{\tau}$ The given torque vector at joints
T Kinetic energy
V Potential energy
$\mathbf{M}(\mathbf{q})$ Inertia matrix
$\mathbf{C}(\mathbf{q},\dot{\mathbf{q}})$ Coriolis/centripetal vector
$\mathbf{G}(\mathbf{q})$ Gravity vector
$\mathbf{N}(\mathbf{q},\dot{\mathbf{q}})$ Nonlinear terms
J Performance index
$\mathbf{F}(t_f)$ Terminal cost matrix
$\mathbf{Q}(t)$ Error weighted matrix
$\mathbf{R}(t)$ Control weighted matrix
$\mathbf{u}^*(t)$ Optimal control
$\mathbf{K}(t)$ *Kalman gain*
$\mathbf{x}^*$ Optimal state
$\mathbf{K_P}$, $\mathbf{K_I}$ and $\mathbf{K_D}$ PID diagonal coefficients

1 INTRODUCTION

Hand is considered as an agent of human brain and is the most intriguing and versatile appendages to human body. Over the last several yeas, attempts have been made to build a prosthetic hand to replace human hand that fully simulate the various natural/human-like operations of moving, grasping, lifting, twisting and so on. Replicating the human hand in all its various functions is still a challenging task due to the extreme complexity of human hand, which has 27 bones, controlled by about 38 muscles to provide the hand with 22 degrees of freedom (DOFs), and incorporates about 17,000 tactile units of 4 different units [1]. Parallels between dextrous robot and human hands were explored by examining sensor motor integration in the design and control of these robots by bringing together experimental psychologists, kinesiologists, computer scientists, and electrical and mechanical engineers.

Artificial hands, developed by various researchers in the field [1–4], have been around for the last several years. However, about 35% of the amputees [5] do not use their prosthetic hand regularly due to various reasons such as poor functionality of the presently available prosthetic hands and psychological problems. To overcome this problem, one has to design and develop an artificial hand which "mimics the human hand as closely as possible" both in functionality and appearance.

Soft computing/control (SC) or computational intelligence (CI) [6] is an emerging field based on synergy and seamless integration of neural networks (NN), fuzzy logic (FL) and genetic algorithms (GA) [7]. The previous works on prosthetic hand used artificial NNs [8], FL [9], GA [10] etc. mostly for EMG signal classification for various movements or functions of the prosthetic hand. Hard computing/control (HC) techniques comprise proportional integral derivative (PID) control [11–14], optimal control [15,16], etc. with specific applications to prosthetics. SC can be used at upper levels of the overall mission where human involvement and decision making is of primary importance. HC can be used at lower levels for accuracy, precision, stability and robustness. Therefore, the integration of SC and HC methodologies could solve problems that cannot be solved satisfactorily by using either methodology alone and lead to high performance, robust, autonomous and cost-effective systems.

However, our previous works [13, 14] for smart prosthetic hand showed that PID controller results in the overshooting and oscillation, which were also demonstrated by Subudhi and Morris [11] and Liu et al. [12]. To overcome the problem, fusion of soft computing technique of adaptive neuro-fuzzy inference system (ANFIS) and finite-time linear quadratic optimal control strategy for two-fingered prosthetic hand is precisely the main goal of this work.

In this paper, we first consider briefly the trajectory planning problem and the inverse kinematics for both two-link thumb and three-link index finger using the ANFIS. Next, the dynamics of the hand is derived and feedback linearization technique is used to obtain *linear* tracking error dynamics. Then the hybrid finite-time linear quadratic optimal controller is designed to minimize the tracking error. The resulting overall hybrid system incorporating both soft and hard control techniques is simulated with practical data for the hand. The last section details the conclusions and future work.

2 Modeling

In this section, we present briefly the trajectory planning problem and the inverse kinematics for both two-link thumb and three-link index finger using ANFIS. The dynamics of the hand is also given.

2.1 Trajectory Planning

To generate smooth trajectories, a cubic polynomial function for the fingertip space is created. A time history of desired (d) fingertip positions (p), velocities (v), and accelerations (a) is given as [17]

$$p_d^j(t) = A_0 + A_1 t + A_2 t^2 + A_3 t^3, \tag{1}$$

$$v_d^j(t) = A_1 + 2A_2 t + 3A_3 t^2, \tag{2}$$

$$a_d^j(t) = 2A_2 + 6A_3 t, \tag{3}$$

where, A_0-A_3 are undetermined constants and the superscript j indicates the index of each finger. The relations (1) and (2) need to satisfy the constraint conditions at t_0 and t_f. This can be written as

$$\mathbf{TA} = \mathbf{P}. \tag{4}$$

Here, the matrices **T**, **A**, and **P** are

$$\mathbf{T} = \begin{bmatrix} 1 & t_0 & t_0^2 & t_0^3 \\ 0 & 1 & 2t_0 & 3t_0^2 \\ 1 & t_f & t_f^2 & t_f^3 \\ 0 & 1 & 2t_f & 3t_f^2 \end{bmatrix}, \tag{5}$$

$$\mathbf{A} = \begin{bmatrix} A_0 & A_1 & A_2 & A_3 \end{bmatrix}', \tag{6}$$

$$\mathbf{P} = \begin{bmatrix} p_0^j & v_0^j & p_f^j & v_f^j \end{bmatrix}'. \tag{7}$$

Therefore, the 4 unknown constants, A_0-A_3, can be computed by $\mathbf{A} = \mathbf{T}^{-1}\mathbf{P}$.

2.2 Inverse Kinematics

A desired trajectory is usually specified in *Cartesian* space and the trajectory controller is easily performed in the *joint* space. Hence, it is necessary to convert Cartesian trajectory planning to the joint space [18–21]. Using inverse kinematics, the joint angles of each finger need to be obtained from the known fingertip positions (*joint space*). Then the angular velocities and angular accelerations of each finger can be obtained from the velocities and accelerations of fingertips by the Jocobian.

2.2.1 Two-Link Thumb As shown in Figure 1, the thumb is assumed as a two-link finger and the index finger is considered as a three-link finger. Hence, the joint angles, angular velocities, and angular accelerations of each finger can be deduced as follows.

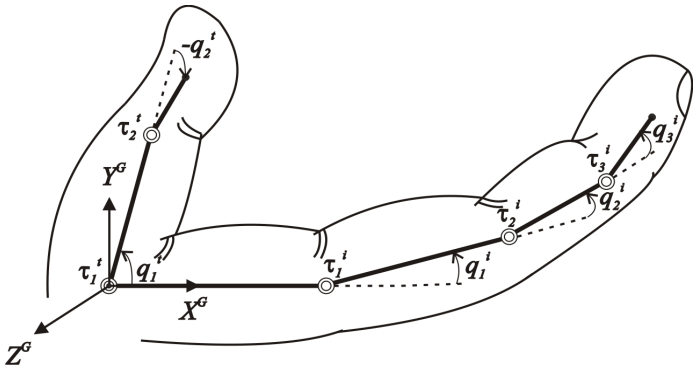

Figure 1. Schematic Diagram of Thumb and Index Finger

According to forward kinematics [22], the fingertip coordinate (X^t, Y^t) of the thumb (t) can be described as

$$X^t = L_1^t \cos(q_1^t) + L_2^t \cos(q_1^t + q_2^t), \tag{8}$$

$$Y^t = L_1^t \sin(q_1^t) + L_2^t \sin(q_1^t + q_2^t). \tag{9}$$

Here L_1^t and L_2^t are the lengths of the links 1 and 2 of the thumb, respectively; q_1^t and q_2^t are the angles of joints 1 and 2 of the thumb. Choosing the *elbow up* configuration, the angle q_2^t of the joint 2 can be obtained as:

$$q_2^t = -\cos^{-1}\left(\frac{X^{t\,2} + Y^{t\,2} - L_1^{t\,2} - L_2^{t\,2}}{2L_1^t L_2^t}\right). \tag{10}$$

Based on the geometry, we can get

$$q_1^t = \tan^{-1}\left(\frac{Y^t}{X^t}\right) - \tan^{-1}\left(\frac{L_2^t \sin(q_2^t)}{L_1^t + L_2^t \cos(q_2^t)}\right). \tag{11}$$

The corresponding velocities $d(X^t, Y^t)/dt$ of the fingertip are obtained as

$$\dot{\mathbf{P}}^t = \mathbf{J}^t \dot{\mathbf{q}}^t, \tag{12}$$

where, the matrices $\dot{\mathbf{P}}^t$ and $\dot{\mathbf{q}}^t$ are

$$\dot{\mathbf{P}}^t = \begin{bmatrix} \dot{X}^t \\ \dot{Y}^t \end{bmatrix}, \quad \dot{\mathbf{q}}^t = \begin{bmatrix} \dot{q}_1^t \\ \dot{q}_2^t \end{bmatrix}. \tag{13}$$

The matrix $\mathbf{J}^t$ is called the *Jacobian* of the thumb and the angular velocities $\dot{q}_1^t$ and $\dot{q}_2^t$ of the joints 1 and 2 are

$$\dot{\mathbf{q}}^t = \mathbf{J}^{t\,-1} \dot{\mathbf{P}}^t. \tag{14}$$

Similarly, the angular accelerations $\ddot{q}_1^t$ and $\ddot{q}_2^t$ of the joints 1 and 2 are obtained as

$$\ddot{\mathbf{q}}^t = \mathbf{J}^{t\,-1}\left(\ddot{\mathbf{P}}^t - \frac{d\mathbf{J}^t}{d\mathbf{t}}\dot{\mathbf{q}}^t\right), \tag{15}$$

where $\ddot{\mathbf{P}}^t$ is the acceleration vector of the fingertip. $\ddot{\mathbf{P}}^t$ and $\ddot{\mathbf{q}}^t$ are denoted as

$$\ddot{\mathbf{P}}^t = \begin{bmatrix} \ddot{X}^t \\ \ddot{Y}^t \end{bmatrix}, \quad \ddot{\mathbf{q}}^t = \begin{bmatrix} \ddot{q}_1^t \\ \ddot{q}_2^t \end{bmatrix}. \tag{16}$$

2.2.2 Three-Link Index Finger As shown in Figure 2, the fingertip Cartesian coordinates (X^i, Y^i) of the index finger (i) are described in terms of three joint variables q_1^i, q_2^i, and q_3^i as

$$\begin{aligned} X^i &= d + L_1^i \cos(q_1^i) + L_2^i \cos(q_1^i + q_2^i) + L_3^i \cos(q_1^i + q_2^i + q_3^i), \\ Y^i &= L_1^i \sin(q_1^i) + L_2^i \sin(q_1^i + q_2^i) + L_3^i \sin(q_1^i + q_2^i + q_3^i). \end{aligned} \tag{17}$$

Here, based on practical data, the relation $q_3^i = 0.7q_2^i$ is used [3] to solve redundancy in the plane x-y in Figure 2. Using this

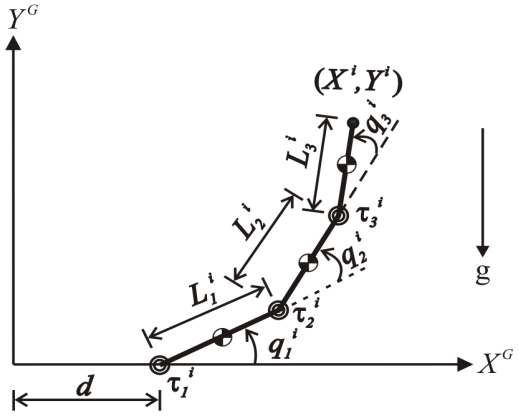

Figure 2. Three-Link Index Finger Illustration

relation into (17), the resulting nonlinear functions are solved by numerical methods, such as Newton-Raphson [23] and the hybrid particle swarm optimization neural network (HPSONN) by Wen et al. [24]. Now, setting up the two functions f_1^i and f_2^i of the two variables q_1^i and q_2^i, we get

$$\begin{aligned} f_1^i &= d + L_1^i \cos(q_1^i) + L_2^i \cos(q_1^i + q_2^i) \\ &\quad + L_3^i \cos(q_1^i + 1.7q_2^i) - X^i, \end{aligned} \tag{18}$$

$$\begin{aligned} f_2^i &= L_1^i \sin(q_1^i) + L_2^i \sin(q_1^i + q_2^i) \\ &\quad + L_3^i \sin(q_1^i + 1.7q_2^i) - Y^i. \end{aligned} \tag{19}$$

This becomes an optimal (minimization) problem with two objective functions f_1^i and f_2^i with two variables q_1^i and q_2^i. The variables ${q_1^i}^*$ and ${q_2^i}^*$ are searched to make the two objective functions f_1^i and f_2^i be close to zero using genetic algorithm, then ${q_1^i}^*$, ${q_2^i}^*$, and ${q_3^i}^* (= 0.7{q_2^i}^*)$ are the solutions of the joint angles of the fingertip coordinate (X^i, Y^i). Alternatively, the inverse kinematics problem can be solved using ANFIS method [25] where the input of the fuzzy-neuro system is the Cartesian space and the output is the joint space. During our simulations [14], we found that the GA method although give a better solution (error $\approx 10^{-7}$), takes more execution time whereas the ANFIS gave a good solution (error $\approx 10^{-4}$) with less time compared to GA method. Once we found the angular positions as above, then, similar to two-link thumb, all angular velocities and accelerations of the joints of the index finger can be calculated.

2.3 Dynamics of Hand

It is necessary to have a mathematical model that describes the dynamic behavior of prosthetic hand for the purpose of designing the control system. The dynamic equations of hand motion are derived via Lagrangian approach using kinetic energy and potential energy as [17, 22, 23]

$$\frac{d}{dt}\left(\frac{\partial \mathcal{L}}{\partial \dot{\mathbf{q}}}\right) - \frac{\partial \mathcal{L}}{\partial \mathbf{q}} = \boldsymbol{\tau}, \tag{20}$$

where $\mathcal{L}$ is the Lagrangian; $\dot{\mathbf{q}}$ and $\mathbf{q}$ represent the angular velocity and angle vectors of joints, respectively; $\boldsymbol{\tau}$ is the given torque vector at joints. The Lagrangian $\mathcal{L}$ can be expressed as

$$\mathcal{L} = T - V, \tag{21}$$

where T and V denote kinetic and potential energies, respectively. Substitute (21) into (20) and dynamic equations of thumb can be obtained as below.

$$\mathbf{M}(\mathbf{q})\ddot{\mathbf{q}} + \mathbf{C}(\mathbf{q}, \dot{\mathbf{q}}) + \mathbf{G}(\mathbf{q}) = \boldsymbol{\tau}, \tag{22}$$

where $\mathbf{M}(\mathbf{q})$ is the inertia matrix; $\mathbf{C}(\mathbf{q}, \dot{\mathbf{q}})$ is the Coriolis/centripetal vector and $\mathbf{G}(\mathbf{q})$ is the gravity vector. (22) can be also written as

$$\mathbf{M}(\mathbf{q})\ddot{\mathbf{q}} + \mathbf{N}(\mathbf{q}, \dot{\mathbf{q}}) = \boldsymbol{\tau}, \tag{23}$$

where $\mathbf{N}(\mathbf{q}, \dot{\mathbf{q}})$ = $\mathbf{C}(\mathbf{q}, \dot{\mathbf{q}})$+$\mathbf{G}(\mathbf{q})$ represents nonlinear terms. The dynamic relations for the two-link thumb and the three-link index finger are quite lengthy and omitted here due to lack of space [21, 26, 27].

3 Control Techniques

3.1 Feedback Linearization

The nonlinear dynamics represented by (23) is to be converted into a linear state-variable system by finding a transformation using feedback linearization technique [17, 28]. Alternative state-space equations of the dynamics can be obtained by defining the position/velocity state $\mathbf{x}(t)$ of the joints as

$$\mathbf{x}(t) = \begin{bmatrix} \mathbf{q}(t)' & \dot{\mathbf{q}}(t)' \end{bmatrix}'. \tag{24}$$

Let us repeat the dynamical model and rewrite (23) as

$$\frac{d}{dt}\dot{\mathbf{q}}(t) = -\mathbf{M}(\mathbf{q}(t))^{-1}\mathbf{N}(\mathbf{q}(t), \dot{\mathbf{q}}(t)) + \mathbf{M}(\mathbf{q}(t))^{-1}\boldsymbol{\tau}(t). \tag{25}$$

Thus, from (24) and (25), we can derive a linear state-variable equation in *Brunovsky canonical form* as

$$\dot{\mathbf{x}}(t) = \begin{bmatrix} \mathbf{0} & \mathbf{I} \\ \mathbf{0} & \mathbf{0} \end{bmatrix} \mathbf{x}(t) + \begin{bmatrix} \mathbf{0} \\ \mathbf{I} \end{bmatrix} \mathbf{u}(t) \tag{26}$$

with its control input vector given by

$$\mathbf{u}(t) = -\mathbf{M}(\mathbf{q}(t))^{-1}\mathbf{N}(\mathbf{q}(t), \dot{\mathbf{q}}(t)) + \mathbf{M}(\mathbf{q}(t))^{-1}\boldsymbol{\tau}(t). \tag{27}$$

Let us suppose the prosthetic hand is required to track the desired trajectory $\mathbf{q}_d(t)$ described under path generation or tracking. Then, the tracking error $\mathbf{e}(t)$ is defined as

$$\mathbf{e}(t) = \mathbf{q}_d(t) - \mathbf{q}(t). \tag{28}$$

Here, $\mathbf{q}_d(t)$ is the *desired* angle vector of joints and can be obtained by (1), (10) and (11); $\mathbf{q}(t)$ is the *actual* angle vector of joints. Differentiating (28) twice, to get

$$\dot{\mathbf{e}}(t) = \dot{\mathbf{q}}_d(t) - \dot{\mathbf{q}}(t), \quad \ddot{\mathbf{e}}(t) = \ddot{\mathbf{q}}_d(t) - \ddot{\mathbf{q}}(t). \tag{29}$$

Substituting (24) into (29) yields

$$\ddot{\mathbf{e}}(t) = \ddot{\mathbf{q}}_d(t) + \mathbf{M}(\mathbf{q}(t))^{-1}(\mathbf{N}(\mathbf{q}(t), \dot{\mathbf{q}}(t)) - \boldsymbol{\tau}(t)) \tag{30}$$

from which the control function can be defined as

$$\mathbf{u}(t) = \ddot{\mathbf{q}}_d(t) + \mathbf{M}(\mathbf{q}(t))^{-1}(\mathbf{N}(\mathbf{q}(t), \dot{\mathbf{q}}(t)) - \boldsymbol{\tau}(t)). \tag{31}$$

This is often called the *feedback linearization* control law, which can also be inverted to express it as

$$\boldsymbol{\tau}(t) = \mathbf{M}(\mathbf{q}(t))(\ddot{\mathbf{q}}_d(t) - \mathbf{u}(t)) + \mathbf{N}(\mathbf{q}(t), \dot{\mathbf{q}}(t)). \tag{32}$$

Using the relations (29) and (31), and defining state vector $\mathbf{x}(t) = [\mathbf{e}(t)' \quad \dot{\mathbf{e}}(t)']'$, the *tracking error dynamics* can be written as

$$\dot{\mathbf{x}}(t) = \begin{bmatrix} \mathbf{0} & \mathbf{I} \\ \mathbf{0} & \mathbf{0} \end{bmatrix} \mathbf{x}(t) + \begin{bmatrix} \mathbf{0} \\ \mathbf{I} \end{bmatrix} \mathbf{u}(t). \tag{33}$$

Note that this is in the form of a *linear* system such as

$$\dot{\mathbf{x}}(t) = \mathbf{A}\mathbf{x}(t) + \mathbf{B}\mathbf{u}(t). \tag{34}$$

Thus, we use the liearized system (34) to minimize the tracking error (28).

3.2 Hybrid Finite-Time Linear Quadratic Optimal Control

Figure 3 shows the block diagram of a hybrid finite-time linear quadratic optimal controller. For the linear system (34), we can formulate the well-known finite-time linear quadratic optimal control problem by defining a performance index J [16] such as

$$J = \frac{1}{2}\mathbf{x}'(t_f)\mathbf{F}(t_f)\mathbf{x}(t_f) + \frac{1}{2}\int_{t_0}^{t_f} \left[\mathbf{x}'(t)\mathbf{Q}(t)\mathbf{x}(t) + \mathbf{u}'(t)\mathbf{R}(t)\mathbf{u}(t)\right] dt, \tag{35}$$

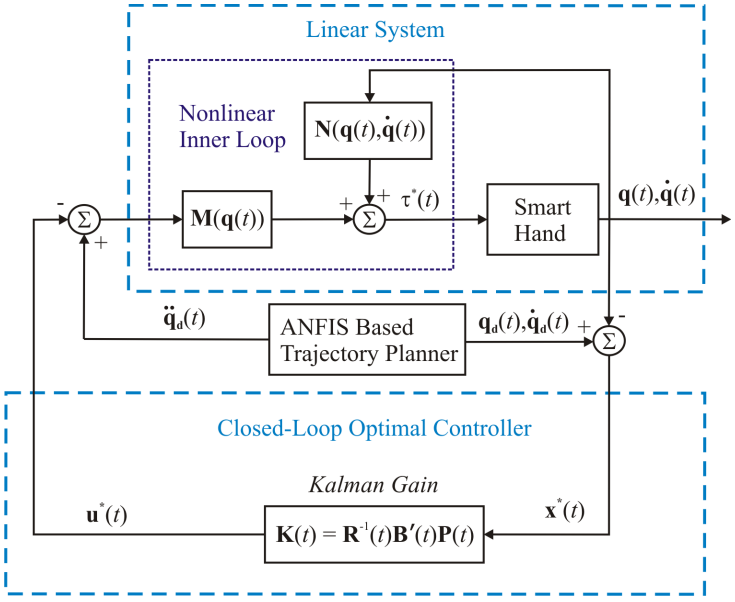

Figure 3. Block Diagram of Hybrid Optimal Controller for Prosthetic Hand

where the terminal cost matrix $\mathbf{F}(t_f)$ and the error weighted matrix $\mathbf{Q}(t)$ are positive *semidefinite* matrices, respectively; the control weighted matrix $\mathbf{R}(t)$ is a positive *definite* matrix. The optimal control $\mathbf{u}^*(t)$ is given by

$$\mathbf{u}^*(t) = -\mathbf{R}^{-1}(t)\mathbf{B}'\mathbf{P}(t)\mathbf{x}^*(t) = -\mathbf{K}(t)\mathbf{x}^*(t). \tag{36}$$

Here, $\mathbf{K}(t) = \mathbf{R}^{-1}(t)\mathbf{B}'\mathbf{P}(t)$ is called *Kalman gain* and $\mathbf{P}(t)$, the symmetric *positive definite* matrix (for all $t \in [t_0, t_f]$), is the solution of the matrix differential Riccati equation (DRE)

$$\dot{\mathbf{P}}(t) = -\mathbf{P}(t)\mathbf{A} - \mathbf{A}'\mathbf{P}(t) - \mathbf{Q}(t) + \mathbf{P}(t)\mathbf{B}\mathbf{R}^{-1}(t)\mathbf{B}'\mathbf{P}(t) \tag{37}$$

satisfying the *final* condition

$$\mathbf{P}(t = t_f) = \mathbf{F}(t_f). \tag{38}$$

The optimal state $\mathbf{x}^*$ is the solution of

$$\dot{\mathbf{x}}^*(t) = \left[\mathbf{A} - \mathbf{B}\mathbf{R}^{-1}(t)\mathbf{B}'\mathbf{P}(t)\right]\mathbf{x}^*(t). \tag{39}$$

Therefore, the required torque $\boldsymbol{\tau}^*(t)$ can be calculated by the optimal control $\mathbf{u}^*(t)$.

$$\boldsymbol{\tau}^*(t) = \mathbf{M}(\mathbf{q}(t))(\ddot{\mathbf{q}}_d(t) - \mathbf{u}^*(t)) + \mathbf{N}(\mathbf{q}(t), \dot{\mathbf{q}}(t)). \tag{40}$$

We also intend to use infinite-time optimal regulator to avoid backward integration of the DRE, especially for on-line (real-time) design and implementation.

4 Simulation Results and Discussion

When thumb and fingers are doing extension/flexion movements, the ranges that fingertips can reach are restricted to the reach of the angles of the joints. Referring to inverse kinematics, Figure 4 shows the workspace of the fingertips of thumb (pink)

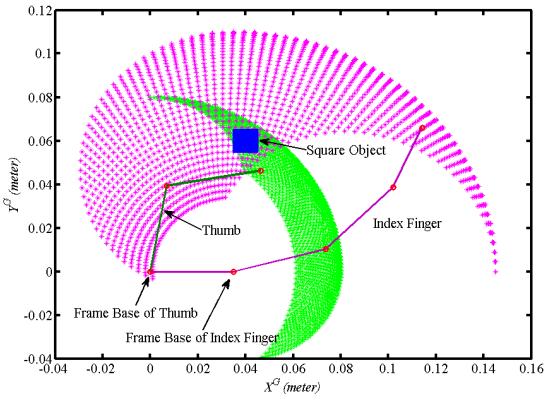

Figure 4. The Workspace of the Fingertips of Thumb and Index Finger with a Square Object

and index finger (green) and a square object (blue). The first and second joint angles of the thumb are constrained in the ranges of [0,90] and [-80,0] (degrees). The first, second, and third joint angles of the index finger are constrained in the ranges of [0,90], [0,110] and [0,80] (degrees), respectively [29]. Thus, the green and pink regions respectively show the reachable fingertip positions of thumb and index finger. Further, the overlap region represents that the space that both the thumb and the index finger can reach.

Next, we present simulations with a PID controller [14,21] and finite-time linear quadratic optimal control for the two-link thumb and three-link index finger of a smart prosthetic hand. The various parameters [30] relating to desired trajectory and the two-link thumb/three-link index finger selected for the simulations are given in Table 1 and the side length of the target square-shaped object is 0.010 (m). All initial actual angles are zero and PID diagonal coefficients, $\mathbf{K_P}$, $\mathbf{K_I}$ and $\mathbf{K_D}$, are 100. As for optimal control coefficients, $\mathbf{A}$, $\mathbf{B}$, $\mathbf{F}(t_f)$, $\mathbf{R}(t)$ and $\mathbf{Q}(t)$ of thumb and index finger are respectively chosen as

$$\mathbf{A} = \begin{bmatrix} \mathbf{0} & \mathbf{I} \\ \mathbf{0} & \mathbf{0} \end{bmatrix}, \quad \mathbf{B} = \begin{bmatrix} \mathbf{0} \\ \mathbf{I} \end{bmatrix}, \quad \mathbf{F}(t_f) = \mathbf{I}, \quad \mathbf{R}(t) = \frac{1}{30}\mathbf{I},$$

$$\mathbf{Q}(t)^t = \begin{bmatrix} \mathbf{Q_{11}} & \mathbf{Q_{12}} \\ \mathbf{Q_{12}} & \mathbf{Q_{22}} \end{bmatrix}, \quad \mathbf{Q}(t)^i = \begin{bmatrix} \mathbf{Q_{11}} & \mathbf{Q_{12}} & \mathbf{Q_{13}} \\ \mathbf{Q_{12}} & \mathbf{Q_{22}} & \mathbf{Q_{23}} \\ \mathbf{Q_{13}} & \mathbf{Q_{23}} & \mathbf{Q_{33}} \end{bmatrix},$$

$$\mathbf{Q_{11}} = \begin{bmatrix} 10 & 2 \\ 2 & 10 \end{bmatrix}, \quad \mathbf{Q_{22}} = \begin{bmatrix} 30 & 0 \\ 0 & 30 \end{bmatrix}, \quad \mathbf{Q_{33}} = \begin{bmatrix} 20 & 1 \\ 1 & 20 \end{bmatrix},$$

$$\mathbf{Q_{12}} = \begin{bmatrix} -4 & 4 \\ 3 & -6 \end{bmatrix}, \mathbf{Q_{13}} = \begin{bmatrix} -4 & 4 \\ 3 & -6 \end{bmatrix}, \mathbf{Q_{23}} = \begin{bmatrix} -4 & 3 \\ 4 & -6 \end{bmatrix}.$$

The first term of the right side in (35) can be neglected by using $\mathbf{F}(t_f)$ as the zero matrix. In this work, there is no significant difference. Figures 5 and 6 show the simulations with PID controller while Figures 7 and 8 the simulations with presented finite-time optimal control method. It is clearly seen that the results using proposed optimal control method can overcome the overshooting and oscillation problems.

Table 1. Parameter Selection of the Smart Hand

Parameters	Values
Thumb	
Time (t_0, t_f)	0, 20 (sec)
Desired Initial Position (X_0^t, Y_0^t)	0.035, 0.060 (m)
Desired Final Position (X_f^t, Y_f^t)	0.0495, 0.060 (m)
Desired Initial Velocity ($\dot{X}_0^t$, $\dot{Y}_0^t$)	0, 0 (m/s)
Desired Final Velocity ($\dot{X}_f^t$, $\dot{Y}_f^t$)	0, 0 (m/s)
Length (L_1^t, L_2^t)	0.040, 0.040 (m)
Mass (m_1^t, m_2^t)	0.043, 0.031 (kg)
Inertia (I_{zz1}^t, I_{zz2}^t)	6.002×10^{-6}, 4.327×10^{-6} (kg-m^2)
Index Finger	
Desired Initial Position (X_0^i, Y_0^i)	0.065, 0.080 (m)
Desired Final Position (X_f^i, Y_f^i)	0.010, 0.060 (m)
Desired Initial Velocity ($\dot{X}_0^i$, $\dot{Y}_0^i$)	0, 0 (m/s)
Desired Final Velocity ($\dot{X}_f^i$, $\dot{Y}_f^i$)	0, 0 (m/s)
Length (L_1^i, L_2^i, L_3^i)	0.040, 0.040, 0.030 (m)
Mass (m_1^i, m_2^i, m_3^i)	0.045, 0.025, 0.017 (kg)
Inertia (I_{zz1}^i, I_{zz2}^i, I_{zz3}^i)	9.375×10^{-6}, 3.333×10^{-6}, 1.125×10^{-6} (kg-m^2)

5 Conclusions and Future Works

This paper focussed on a hybrid of soft computing or control technique of adaptive neuro-fuzzy inference system (ANFIS) and a hard computing or control technique of finite-time linear quadratic optimal control for a two-fingered (thumb and index) prosthetic hand. In particular, the ANFIS was used for inverse kinematics, and the optimal control was used for feedback linearized dynamics to minimize tracking error. The simulations

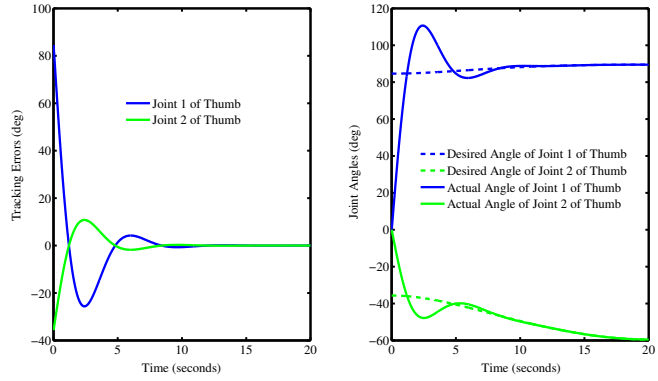

Figure 5. Tracking Errors (left) and Joint Angles (right) for PID Controller of Thumb

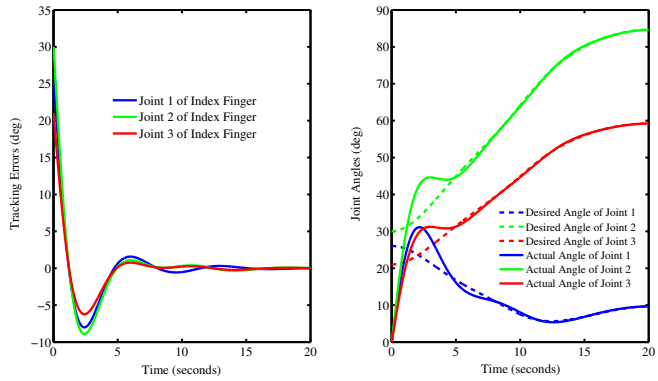

Figure 6. Tracking Errors (left) and Joint Angles (right) for PID Controller of Index Finger

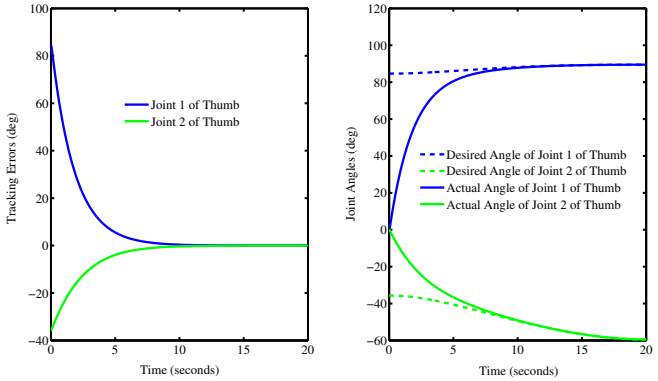

Figure 7. Tracking Errors (left) and Joint Angles (right) for Proposed Optimal Control of Thumb

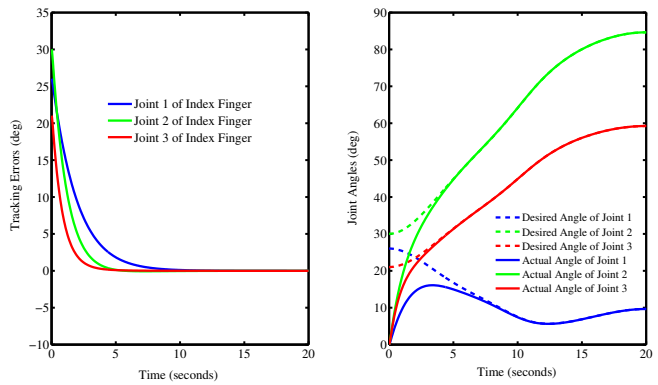

Figure 8. Tracking Errors (left) and Joint Angles (right) for Proposed Optimal Control of Index Finger

of this hybrid controller, when compared with the proportional-integral-derivative (PID) controller showed enhanced performance. Work is underway to extend this methodology to five-fingered, three-dimensional prosthetic hand.

ACKNOWLEDGMENT

The financial support for this research from the Telemedicine Advanced Technology Research Center (TATRC) of the US Department of Defense (DoD) is acknowledged.

REFERENCES

[1] Zecca, M., Micera, S., Carrozza, M., and Dario, P., 2002. "Control of multifunctional prosthetic hands by processing the electromyographic signal". *Critical Reviews^{TM} in Biomedical Engineering,* **30**, pp. 459–485. (Review article with 96 references).

[2] Lai, J. C. K., Schoen, M. P., Perez-Gracia, A., Naidu, D. S., and Leung, S. W., 2007. "Prosthetic devices: Challenges and implications of robotic implants and biological interfaces". *Proceedings of the Institute of Mechanical Engineers (IMechE), Part H: Journal of Engineering in Medicine,* **221**(2), January, pp. 173–183. Special Issue on Micro and Nano Technologies in Medicine.

[3] Zollo, L., Roccella, S., Guglielmelli, E., Carrozza, M. C., and Dario, P., 2007. "Biomechatronic design and control of an anthropomorphic artificial hand for prosthetic and robotic applications". *IEEE/ASME Transactions on Mechatronics,* **12**(4), August, pp. 418–429.

[4] Naidu, D. S., Chen, C.-H., Perez, A., and Schoen, M. P., 2008. "Control strategies for smart prosthetic hand technology: An overview". In Proceedings of the 30th Annual International IEEE EMBS Conference, pp. 4314–4317.

[5] Atkins, D. J., Heard, D. C. Y., and Donovan, W. H., 1996. "Epidemiologic overview of individuals with upper limb loss and their reported research priorities". *Journal of Prosthetic and Orthotics,* **8**(1), pp. 2–11.

[6] Konar, A., 2005. *Computational Intelligence: Principles, Techniques and Applications*. Springer-Verlag, Berlin, Ger-

many.

[7] Karray, F., and De Silva, C., 2004. *Soft Computing and Intelligent Systems Design: Theory, Tools and Applications*. Pearson Educational Limited, Harlow, England, UK.

[8] Light, C. M., Chappell, P. H., Hudgins, B., and Engelhart, K., 2002. "Intelligent multifunction myoelectric control of hand prostheses". *Journal of Medical Engineering & Technology,* **26**(4), July-August, pp. 139–146.

[9] Ajiboye, A. B., and Weir, R. F., 2005. "A heuristic fuzzy logic approach to EMG pattern recognition for multifunctional prosthesis control". *IEEE Transactions on Neural Systems and Rehabilitation Engineering,* **13**(3), September, pp. 280–291.

[10] Fernandez, J. J., Farry, K. A., and Cheatham, J. B., 2000. "Waveform recognition using genetic programming: The myoelectric signal recognition problem". In Proceedings of the first Annual Conference of Genetic Programming, pp. 1754–1759.

[11] Subudhi, B., and Morris, A. S., 2009. "Soft computing methods applied to the control of a flexible robot manipulator". *Applied Soft Computing,* **9**, pp. 149–158.

[12] Liu, F., and Chen, H., 2008. "Motion control of intelligent underwater robot based on cmac-pid". In Proceedings of the 2008 IEEE International Conference on Information and Automation.

[13] Chen, C.-H., Bosworth, K. W., Schoen, M. P., Bearden, S. E., Naidu, D. S., and Perez, A., 2008. "A study of particle swarm optimization on leukocyte adhesion molecules and control strategies for smart prosthetic hand". In 2008 IEEE Swarm Intelligence Symposium (IEEE SIS08).

[14] Chen, C.-H., Naidu, D. S., Perez, A., and Schoen, M. P., 2008. "Fusion of hard and soft control techniques for prosthetic hand". In Proceedings of the International Association of Science and Technology for Development (IASTED) International Conference on Intelligent Systems and Control (ISC 2008), pp. 120–125.

[15] Vrabie, D., Lewis, F., and Abu-Khalaf, M., 2008. "Biologically inspired scheme for continuous-time approximate dynamic programming". *Transactions of the Institute of Measurement and Control,* **30**, pp. 207–223.

[16] Naidu, D., 2003. *Optimal Control Systems*. CRC Press, Boca Raton, FL.

[17] Lewis, F., Dawson, D., and Abdallah, C., 2004. *Robot Manipulators Control: Second Edition, Revised and Expanded*. Marcel Dekker, Inc.,, New York, NY.

[18] Kelly, R., Santibanez, V., and Loria, A., 2005. *Control of Robot Manipulators in Joint Space*. Springer, New York, USA.

[19] Jazar, R. N., 2007. *Theory of Applied Robotics. Kinematics, Dynamics, and Control*. Springer, New York, USA.

[20] Siciliano, B., Sciavicco, L., Villani, L., and Oriolo, G., 2009. *Robotics: Modelling, Planning and Control*. Springer-Verlag, London, UK.

[21] Chen, C.-H., 2009. "Hybrid control strategies for smart prosthetic hand". PhD thesis, Measurement and Control Engineering, Idaho State University, May.

[22] R. Kelly, V. S., and Loria, A., 2005. *Control of Robot Manipulators in Joint Space*. Springer, New York, USA.

[23] Jazar, R. N., 2007. *Theory of Applied Robotics. Kinematics, Dynamics, and Control*. Springer, New York, USA.

[24] Wen, X., Sheng, D., and Huang, J., 2008. *A Hybrid Particle Swarm Optimization for Manipulator Inverse Kinematics Control*, Vol. 5226 of *Lecture Notes in Computer Science*. Springer-Verlag, Berlin, Heidelberg.

[25] Jang, J.-S., Sun, C.-T., and Mizutani, E., 1997. *Neuro-Fuzzy and Soft Computing: A Computational Approach to Learning and Machine Intelligence*. Prentice Hall PTR, Upper Saddle River, NJ.

[26] Nikoobin, A., and Haghighi, R., 2008. "Lyapunov-based nonlinear disturbance observer for serial n-link robot manipulators". *Journal of Intelligent and Robotic Systems*. (Published online on 11 December 2008).

[27] Arslan, Y. Z., Hacioglu, Y., and Yagiz, N., 2008. "Prosthetic hand finger control using fuzzy sliding modes". *Journal of Intelligent and Robotic Systems,* **52**, pp. 121–138.

[28] Marquez, M., 2003. *Nonlinear Control Systems: Analysis and Design*. Wiley-Interscience, Hoboken, NJ.

[29] Lavangie, P. K., and Norkin, C. C., 2001. *Joint Structure and Function: A Comprehensive Analysis, Third Edition*. F. A. Davis Company, Philadelphia, PA.

[30] Arimoto, S., 2008. *Control Theory of Multi-fingered Hands: A Modeling and Analytical-Mechanics Approach for Dexterity and Intelligence*. Springer-Verlag, London, UK.